Journal of Smart Sensor and Materials
Volume 4, No. 1, 2026 1-13

FLUORESCENT SILICON QUANTUM DOTS FOR THE DETECTION OF URIC ACID

Hassan Grema[1], Jaafar Abdullah[1,2*] and Nor Azah Yusof[1,2]

[1]Department of Chemistry, Faculty of Science, Universiti Putra Malaysia, 43400 UPM Serdang, Selangor, Malaysia.
[2]Institute of Nanoscience and Nanotechnology (ION2), University Putra Malaysia, 43400 Serdang, Selangor, Malaysia
**Corresponding author email: jafar@upm.edu.my*

Abstract

Silicon quantum dots (SiQDs) have become one of the most popular nanomaterials with outstanding optical properties, chemical photostability, biocompatibility, water solubility, dispersibility, and ultra-small size. Recently, there has been considerable interest in the application of SiQDs in the development of chemical sensors for healthcare applications. Elevated uric acid levels (hyperuricemia) are clinically associated with pathological conditions such as gout, renal impairment, and cardiovascular complications, thereby necessitating sensitive and reliable detection methods. In this work, a fluorescence sensor based on SiQDs for the detection of uric acid has been described. The SiQDs have been synthesised via one-pot hydrothermal synthesis by reacting 3-aminopropyltriethoxysilane (APTES) as a silicon source, trisodium citrate as a reducing agent, and ethylene diamine as a capping agent. The SiQDs were used as an indicator to reveal the fluorescence property of the system resulting from interactions with uric acid that induced the self-aggregation of the SiQDs and thus quenched the fluorescence intensity. Under optimized conditions, the fluorescence sensor response towards uric acid in the concentration range of 0.004 to 0.100 mg/ml gave linearity ($y = 23346x + 3599.2$, $R^2 = 0.980$) and a limit of detection (LOD) of 0.003 mg/ml. This method is a promising tool for monitoring various diseases, including gout and other diseases.

Keywords: Fluorescence, Quenching, Uric acid, Quantum dots, Sensing

Article History:- Received: 10 March 2026; Revised: 3 April 2026; Accepted: 15 April 2026; Published: 30 April 2026

Introduction

Uric acid ($C_6H_4N_4O_3$) is a substance formed as a byproduct of the breakdown of purine derivatives during human metabolism. Various tissues within the body, such as the endothelium, kidneys, liver, intestines, and muscles, contribute to the production of uric acid. While the primary route of uric acid elimination is through the kidneys, humans lack the uricase enzyme, impeding the conversion of uric acid into a more water-soluble compound and resulting in its presence in urine. The kidneys reabsorb approximately 90% of the filtered uric acid, emphasizing its crucial physiological role. Additionally, uric acid serves as a notable antioxidant, contributing to over half of the antioxidant activity in the plasma (Baig et al., 2022).

Gout manifests when an individual experiences elevated uric acid levels in both their serum and urine. The kidneys play a crucial role in blood purification by excreting the soluble form of uric acid. Elevated uric acid levels can give rise to various health issues, including gout, kidney stones, heart failure, diabetes, high cholesterol, and high blood pressure. Conversely, insufficient uric acid in the bloodstream may contribute to atherosclerosis and stroke, emphasizing the

significance of regulating uric acid levels for overall health. In men, the typical range of uric acid in the bloodstream falls between 3.5 and 7.2 mg/dL, while in women, it ranges from 2.6 to 6 mg/dL. Urine generally contains higher concentrations of uric acid than blood, typically ranging from 25 to 74 mg/dL. The careful monitoring and maintenance of appropriate uric acid concentrations have become imperative for ensuring human well-being (Yaacob et al., 2020).

Hyperuricemia is defined as high levels of uric acid in the blood, and it has been linked to hypertension, metabolic syndrome, and cardiovascular disease. As a result, rapid and accurate measurement of uric acid in biological fluids is commonly required for diagnosis and treatment. Offer provided the first method for uric acid analysis in 1894. This approach is based on the chemical oxidation of uric acid to allantoin, which converts phosphotungstic acid to a tungsten blue chromophoric molecule. However, this approach has various flaws, most notably the problem of interference caused by other species capable of performing the same reaction (Erden & Kiliç, 2013).

It is of utmost importance to identify one's health condition early on through timely medical screening. A variety of health screening methods are available, ranging from self-monitoring to evaluations conducted by healthcare professionals. These methods can be broadly classified as either invasive or non-invasive. Invasive approaches often involve pricking the fingertip to extract blood, which can sometimes lead to calluses, scarring, and discomfort. On the other hand, non-invasive methods utilize alternative body fluids such as saliva, sweat, urine, or tears for healthcare monitoring. These fluids frequently contain disease-related biomarkers and offer a more accessible means of assessment. Using such fluids helps mitigate the drawbacks associated with drawing blood during medical examinations (Azmi et al., 2018).

Various methods have been documented for the analysis of uric acid, including fluorescence analysis (Wang et al., 2018), electrochemical assessment (Tukimin et al., 2017), HPLC-UV detection (Pleskacova et al., 2017), surface-enhanced Raman scattering, and enzymatic-UV detection (Westley et al., 2017). Among these, fluorescence analysis is considered the most efficient for uric acid detection due to its straightforward procedure, rapid results, heightened sensitivity, and cost-effectiveness. However, many fluorescence-based approaches require the presence of uricase to examine the specific substances generated by its catalytic reaction. Since enzymes are both delicate and expensive, it is crucial to develop robust and cost-effective non-enzymatic fluorescence techniques for the detection of uric acid (Zheng et al., 2021).

Silicon quantum dots with zero dimensions (SiQDs) have attracted considerable attention, being considered as potential substitutes for semiconductor quantum dots and traditional organic dyes in sensing and bioimaging applications. Notably, carbon dots based on silane exhibit comparable photoluminescence to other fluorescent nanomaterials, while also presenting additional benefits like low or non-toxicity, excellent photo-stability, significant biocompatibility, and abundance in the Earth's resources (Liu et al., 2022). According to published research, these quantum dots are typically synthesized utilizing electrochemical methods (Morozova et al., 2020), microwave techniques (Li et al., 2021; Xuan et al., 2017; Zhou et al., 2022; Li et al., 2019), ultraviolet irradiation (Li et al., 2020, Wu et al., 2015), and hydrothermal (Zhang et al., 2012) either in their original form or after suitable modifications. These methods can produce quantum dots in their natural state or change them to meet certain requirements (Eda et al., 2020).

In this study, the synthesis of SiQDs using 3-aminopropyltriethoxysilane (APTES) as a silicon source, trisodium citrate as a reducing agent, and ethylene diamine as a capping agent via a hydrothermal process has been explored. The resulting SiQDs exhibit notable luminescence and water solubility. Furthermore, the quantum dots enable highly sensitive and selective detection of uric acid. The SiQDs were used as an indicator to reveal the fluorescence response of the system resulting from interactions with uric acid that induced self-aggregation and thus quenched the

fluorescence intensity. The suggested fluorescent approach was successfully applied to detect uric acid, yielding satisfactory results.

Materials and Methods

Reagents and solutions

3-Aminopropyltriethoxysilane (99%), sodium citrate tribasic dihydrate (≥99.0%), and sodium hydroxide were purchased from Sigma–Aldrich (USA), and deionized water was used for the preparation of phosphate buffer (0.1 M). The pH of the buffer solution (pH 7.2) was adjusted using sodium hydroxide (0.1 M). Aqueous solutions were prepared by deionized water (18.2 MΩ. cm, Simplicity, Milli–Q Millipore water purification system). All the reagents were of analytical grade and used without further purification.

Synthesis of SiQDs

The water-soluble fluorescent SiQDs were produced hydrothermally utilizing APTES and sodium citrate as precursors. In a typical experiment, 1.2 g of sodium citrate was dissolved in 25 mL of nitrogen-rich deionized water. Then, 6 mL of APTES was added and mixed well for 10 minutes. The resulting precursor solution was placed in a stainless-steel autoclave and heated to 180 °C for 5 hours. After cooling to ambient temperature, the resulting transparent mixed solution was dialyzed against ultrapure water for 48 hours to remove contaminants such as APTES molecules and sodium citrate. Finally, the produced and purified SiQDs solution was kept at 4 °C for subsequent usage.

Material Characterization of the as-prepared SiQDs

The UV-vis absorption spectra were determined using a UV-visible spectrophotometer (Thermo ScientificTM MultiskanTM GO) at room temperature within the wavelength range of 200-800 nm, whereas the fluorescence spectra were acquired by Tecan, which was equipped with Tecan black 96-well plates and SPARKCONTROL Magellan software. An FT-IR spectrometer (Brucker, ATR FTIR Alpha) was used to determine and evaluate the molecular makeup of molecules bound to nanoparticle surfaces. The surface morphology of the produced SiQDs was studied using a high-resolution transmission electron microscope (HRTEM). X-ray diffraction (XRD) (Shimadzu XRD 6000 Diffractometer cu - K& copper radiation) was used to evaluate the crystallography of the crystals.

Optimization Parameters

The influence of pH buffer on the uric acid detection was investigated using various pH phosphate buffers in the range of pH 7 to 10. For the measurement, Tecan black 96-well plates were used, consisting of 200 µl of phosphate buffer (pH 7, 7.2, 7.4, 8.0, and 10), 50 µl of uric acid (0.006 mg/ml), and SiQDs (0.5 mg/ml) were mixed in a well. Fluorescence emission was recorded using a microplate multimode reader with excitation and emission wavelengths at 305 and 350 nm, respectively.

For the reaction time study, the highest reaction duration between SiQDs (0.5 mg/ml) and uric acid (0.006 mg/ml) was tested in a phosphate buffer pH 7.2, and the fluorescence intensity at different reaction times was recorded. The excitation and emission were fixed at wavelengths of 305 nm and 350 nm, respectively.

Real Sample Analysis

A urine sample was gathered and spun at 10,000 rpm in a centrifuge for 10 minutes to eliminate impurities. Then the urine sample was mixed with a phosphate buffer of pH 7.2 with a ratio of 1:9 (v/v) (1 ml of urine sample to 9 ml of buffer solution). After dilution, the sample was injected with different concentrations of uric acid solution (0.05 and 0.07 mg/ml). Fluorescence emission readings were conducted using a microplate reader, with an excitation wavelength of 305 nm and an emission wavelength of 440 nm, respectively. The measurement was performed in triplicate (n = 3).

Results and Discussion

Material Characterization

In this study, we present a simple, environmentally friendly, and cost-effective method to produce SiQDs in a single step. APTES was used as the silicon source, while sodium citrate served as a reducing agent. During high-temperature heating, trisodium citrate facilitates the reduction of siloxane molecules forming silicon crystal nuclei. Unlike previous studies employing bulk silicon or SiO_2 precursors (Eda et al., 2020; Li et al., 2019), this approach eliminates the need for post-synthesis hydrophilic modification of hydrophobic SiQDs. In this study, the synthesis of water-soluble fluorescent SiQDs involved the incorporation of ethylenediamine (EDA) as a capping agent, which enhanced nanoparticle stability, prevented agglomeration, and improved control of particle size, thereby significantly enhancing the fluorescence properties of the SiQDs. In addition, the use of APTES as a water-soluble silicon source facilitated its reaction with trisodium citrate during the oxidation–reduction process, further enhancing aqueous solubility and photostability. The synthesised SiQDs appeared yellow in solid form and colourless in solution, exhibiting bright blue fluorescence under UV light. As shown in Figure 1, the fluorescence intensity of SiQDs-EDA was approximately 4.5 times higher than that of uncapped SiQDs, confirming the significant role of EDA in enhancing fluorescence performance. These improvements broaden the potential applications of the synthesised SiQDs in bioimaging, sensing, and optoelectronic applications.

The analysis of surface groups and bonding composition in SiQDs was conducted using Fourier Transform Infrared (FTIR) spectroscopy. As illustrated in Figure 2, the absorption peak at 3443 cm^{-1} indicates O-H stretching vibrations (Pan et al., 2022). The peak at 1301 cm^{-1} is attributed to the vibrational motion of the C-N bond, while the one at 2910 cm^{-1} results from the unsaturated stretching vibration of the C-H bond. The signal at 1566 cm^{-1} originates from the stretching vibration of the C-O bond (Liu et al., 2019). Notably, Si-O bending vibrations, crucial for SiQD preparation, contribute to the significant absorbance at 1109 cm^{-1} and 1012 cm^{-1} (Miao et al., 2017). These results indicate the presence of hydroxyl and amino groups on SiQD surfaces, suggesting excellent water solubility. In summary, the SiQDs exhibit remarkable water solubility due to the abundance of functional hydrophilic groups, including hydroxyl and amino groups, on their surfaces.

Journal of Smart Sensor and Materials
Volume 4, No. 1, 2026 1-13

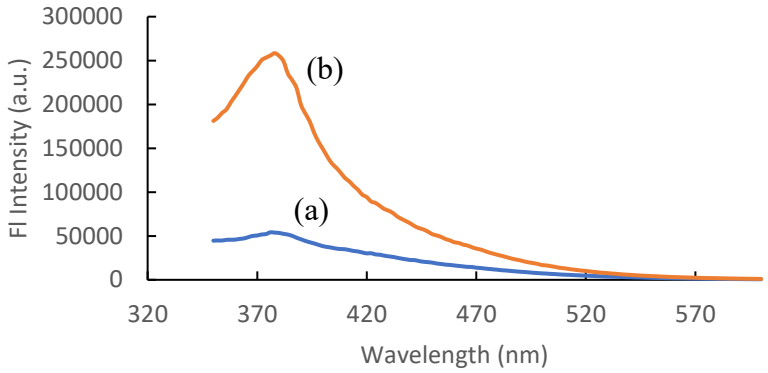

Figure 1. Emission spectra of SiQDs (a) and SiQDs-EDA (b)

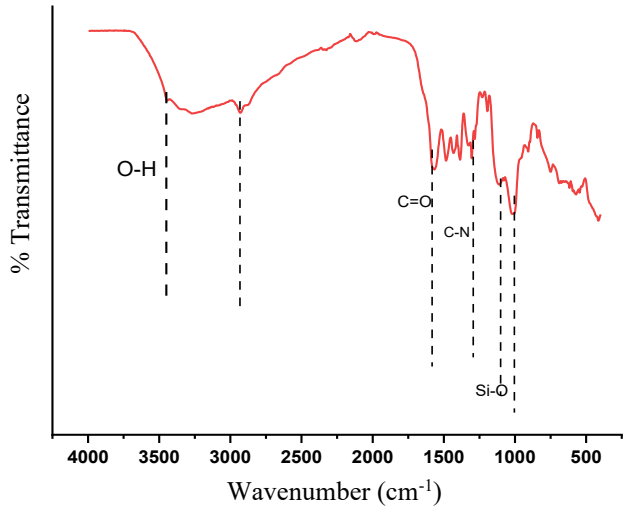

Figure 2. FTIR spectrum of SiQDs

High-resolution transmission electron microscopy (HRTEM) was employed to investigate the morphology and size distribution of SiQDs. As shown in Figure 3, the SiQDs demonstrated uniformity, well-dispersed characteristics, and an almost spherical shape, varying in sizes from 11.81 nm to 12.95 nm. A previous study similarly noted that the SiQDs they prepared exhibited a spherical shape and maintained a nearly uniform size distribution (Eda et al., 2020).

Optical Properties of SiQDs

The optical properties of the produced SiQDs were evaluated using a UV-visible spectrophotometer, UV-visible, and fluorescence techniques. The synthesised colloidal solution of SiQDs, as shown in Figure 4A, has a light-yellow translucent appearance under natural light. However, when exposed to a portable UV lamp, it produced blue fluorescence. A prior study also found that exposure to a UV lamp caused the production of blue fluorescence (Liu et al., 2021).

Journal of Smart Sensor and Materials
Volume 4, No. 1, 2026 1-13

The optical characteristics of SiQDs were investigated by recording the UV-Vis spectrum, as shown in Figure 4B(a). This spectrum shows a continuous pattern of absorption from 200 to 400 nm, with a prominent peak at 329 nm. SiQDs have a broad absorption band in the ultraviolet range, with two distinct peaks at 250 and 350 nm. These peaks represent the π - p* and n - p* transitions of SiQDs, respectively. When exposed to UV light, the SiQDs selectively absorb light at two specific wavelengths: 250 nm and 350 nm. These wavelengths correspond to distinct types of electronic transitions. The π - p* transitions elevate electrons from π orbitals to p* orbitals, whereas the n - p* transitions elevate electrons from non-bonding orbitals to p* orbitals (Xu et al., 2019). Another investigation found a standard absorption band in the UV-Vis absorption spectrum, with two absorption maxima at 280 and 350 nm (Eda et al., 2020).

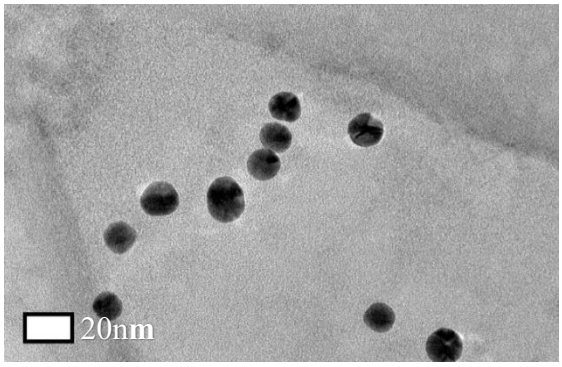

Figure 3. HRTEM image of SiQDs at 20 nm scale

Figure 4B(b) shows the emission parameters of SiQDs. The maximum emission peak of the SiQDs found at 382 nm can be attained when excited at 305 nm, which serves as the optimum excitation wavelength for the following experimental investigations (Liu et al., 2022). Figure 5 illustrates the X-ray diffraction (XRD) analysis, revealing that the SiQDs are predominantly amorphous, as evidenced by a single broad diffraction peak at 2θ = 21.05° (Eda et al., 2020).

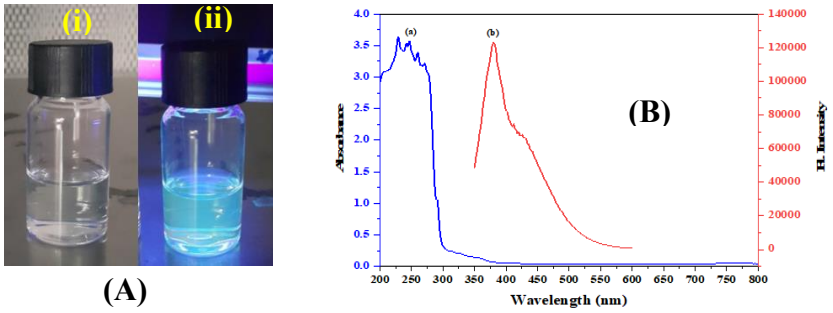

Figure 4. (A) SiQDs under natural light (i) and UV lamp (ii), (B) UV–Vis absorption spectrum (a) and fluorescence emission spectrum (b) of SiQDs

Journal of Smart Sensor and Materials
Volume 4, No. 1, 2026 1-13

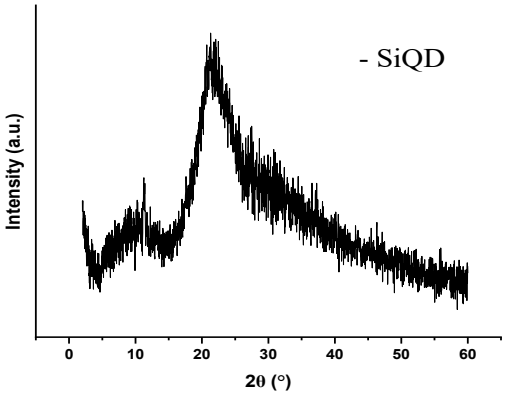

Figure 5. X-ray pattern of the prepared SiQDs

Figure 6 illustrates the possible interaction of SiQDs with uric acid molecules. The synthesized amino-functionalized SiQDs (NH_2@SiQDs) offer good water-solubility, excellent fluorescence property, and optical stability. A non-enzymatic assay of uric acid has been proposed based on the fluorescence quenching of NH_2@SiQDs in response to uric acid. It can be attributed to the fact that uric acid molecules linked to the NH_2@SiQDs together via H-bonding and hydrophobic interactions that induced the self-aggregation of the SiQDs and thus quenched the fluorescence. The fluorescence intensity is inversely proportional to the concentration of uric acid used in the study.

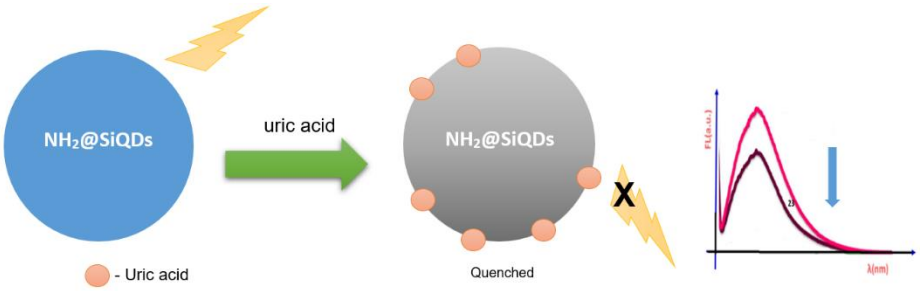

Figure 6. Schematic illustration of the NH_2@SiQDs for sensitive uric acid detection

Optimization parameters

The effect of pH on the fluorescence response for the detection of uric acid is very important, thus, an investigation on the effect of phosphate buffer in the pH range of 7 to 10 was conducted. As can be seen in Figure 7(a), as the pH increased from 7.0 to 7.2, the intensity increased, and above pH 7.2, the intensity started to decrease. The observation can be explained by several factors. At pH 7.2, the SiQDs surface functional groups are in an optimal state, improving fluorescence response. However, higher pH levels can deprotonate the functional groups on SiQDs, thus changing the surface charge and reducing fluorescence response (Azmi et al., 2018; Schrenkhammer, 2008; Tatli et al., 2020). SiQDs are more chemically stable at pH 7.2, while higher pH may cause reactions that lower fluorescence. Lastly, the interaction between SiQDs

Journal of Smart Sensor and Materials
Volume 4, No. 1, 2026 1-13

and uric acid is best at pH 7.2, enhancing fluorescence, whereas higher pH fades this interaction and decreases fluorescence (Agarwal et al., 2023). Previous studies showed that many researchers selected optimum pH values for uric acid that were in the range of 7.0 to 7.5 (Azmi et al., 2018; Schrenkhammer, 2008; Tatli et al., 2020). As can be seen, the buffer indicates that the highest intensity is observed at a buffer with a pH of 7.2. Therefore, phosphate buffer pH 7.2 was chosen as the optimal pH for the detection of uric acid.

Reaction time plays a crucial role in various chemical reactions, impacting their outcomes significantly. Consequently, Figure 7(b) depicts the fluorescence intensity of the SiQDs interacted with uric acid conducted at various time intervals (0−30 min). As shown, the reaction started immediately, and the intensity reached its maximum response at 5 minutes and started declining after 5 minutes of the reaction time. The most favourable outcome was attained at 5 minutes of reaction time. Therefore, the reaction time of 5 minutes was chosen for further study.

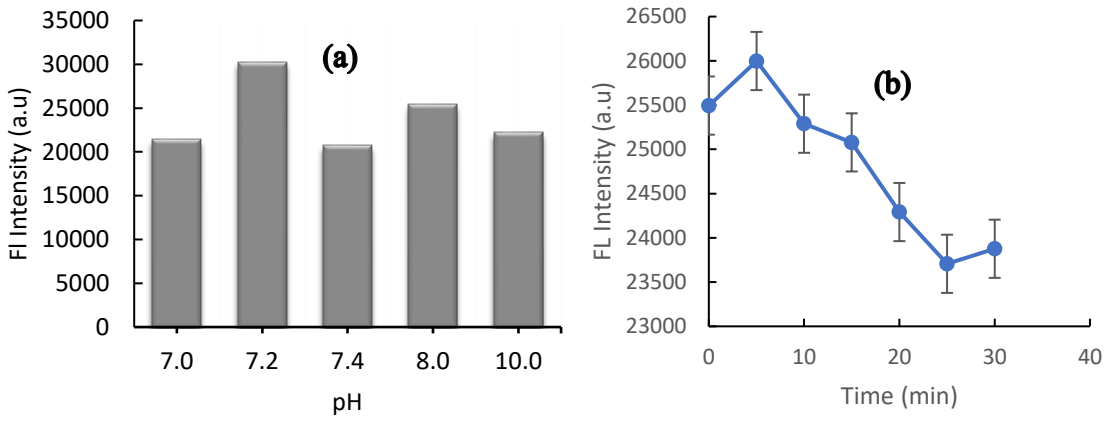

Figure 7. (a) Effect of different pH buffers (b) reaction time. Experimental condition: 0.5 mg/ml of SiQDs and 0.006 mg/ml of uric acid

Analytical performance

The effect of uric acid concentrations on the fluorescence intensity of SiQDs was investigated for uric acid detection. As shown in Figure 8(a), uric acid decreases fluorescence intensity due to quenching of the QDs' fluorescence signal. The graph in Figure 7(b) shows a linear response of fluorescence intensity to uric acid concentration. A good linear correlation was observed for uric acid concentrations of 0.004 to 0.1 mg/ml, with linear regression y = 233467x + 3599.2 (R^2 = 0.980) and a LOD of 0.003 mg/ml. The relatively large error bars observed at some calibration points may be attributed to variations in SiQDs particle size, surface defects, nanoparticle aggregation, and changes in pH or ionic strength, all of which can influence fluorescence quenching efficiency and cause experimental variability (Stephan & Trappitsch, 2023). At lower uric acid concentrations, the fluorescence response becomes more susceptible to instrumental noise and minor experimental deviations, resulting in larger standard deviations. At higher concentrations, partial aggregation of SiQDs or saturation of quenching sites may reduce measurement reproducibility, contributing to calibration variability (Peng et al., 2022).

Journal of Smart Sensor and Materials
Volume 4, No. 1, 2026 1-13

Table 1 illustrates a comparison of the proposed SiQDs-NH_2 (this work) with previously reported systems such as SiQDs/Cu_2-β-CD nanoclusters (Peng et al., 2022) and *Gleditsia sinensis* carbon dots (Kim et al., 2015). The proposed SiQDs–NH_2 probe shows excellent performance, with the widest linearity range (0.004 – 0.100 mg/mL) among the compared methods. Although its LOD (0.003 mg/mL) is slightly higher than previous reports, it remains within the same order of magnitude, demonstrating competitive sensitivity.

Table 1. Comparison of fluorescent probes for uric acid detection

Fluorescent probe	Linearity (mg/ml)	LOD (mg/ml)	Reference
SiQDs/Cu_2-β-CD nanoclusters	0.004-0.025	0.0008	Peng et al., 2022
Gleditsia sinensis carbon dots	0.017-0.084	0.001	Kim et al., 2015
SiQDs-NH_2	0.004-0.100	0.003	This work

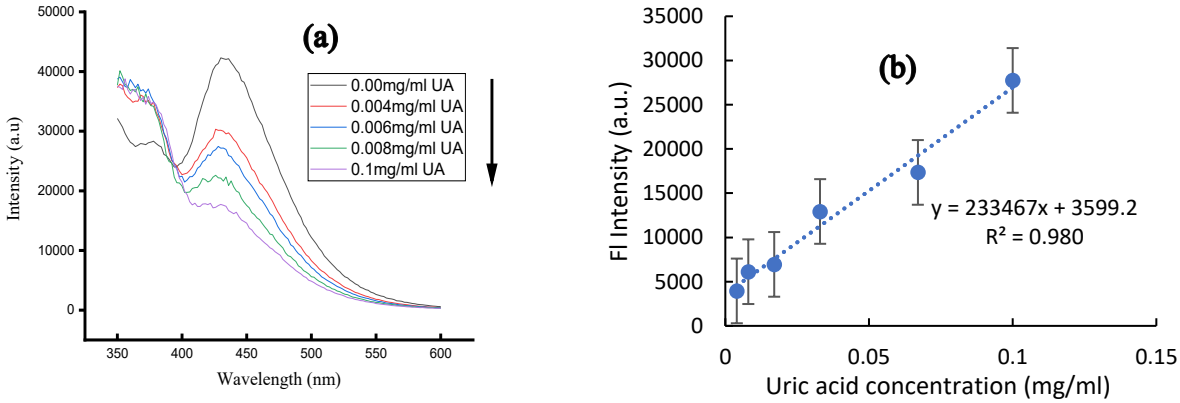

Figure 8. (a) Fluorescence spectra of SiQDs at different uric acid concentrations (b) Calibration curve of fluorescence intensity of SiQDs towards uric acid at different concentrations

The importance of non-enzymatic sensor selectivity cannot be overstated when working with actual biological samples. Therefore, investigating the selectivity of potential interfering substances is essential for sensor development. Several common substances typically found in urine were tested to evaluate their potential impact on the SiQDs' ability to detect uric acid. The changes in the SiQDs' fluorescence intensity were observed in the presence of interfering species. As shown in Table 2, the interference study of common urine constituents on the fluorescence response of the SiQDs sensor. The results revealed that ascorbic acid, creatinine, glucose, urea, KCl, and NaCl caused only slight changes in fluorescence intensity, ranging from −2.4% to 3.9%. While most interfering species showed negligible effects within ±5%, slightly higher deviations were observed for KCl and ascorbic acid, suggesting minor interference. Nevertheless, all variations remained within an acceptable analytical range, indicating good selectivity of the developed SiQDs fluorescence sensor toward uric acid detection in complex urine matrices.

Table 2. Assessment of potential interference in the actual urine sample (n = 3)

Interfering material	Concentration added (mg/ml)	Change fluorescence intensity (%)
Ascorbic acid	0.2	3.8
Creatinine	0.2	1.3
Glucose	0.2	3.6
Urea	0.2	3.4
KCl	0.2	3.9
NaCl	0.2	-2.4

Application of real urine sample

In this study, the practical applicability of the proposed SiQDs sensor for the detection of uric acid in real urine samples was evaluated. As shown in Table 2, no measurable response was observed for the unspiked urine sample. This observation most likely attributed to matrix effects inherent to the complex biological environment of urine (Azizi et al., 2024). Urine contains high concentrations of urea, creatinine, inorganic salts, and other endogenous metabolites that may interfere with the sensing mechanism of the fluorescence quenching. In addition, Table 3 presents the recovery study of a known concentration of uric acid spiked in a urine sample. The results show that the percentage of recoveries was in the range of 98% to 108%. This indicates that the SiQDs sensor has great abilities in fluorescence detection of uric acid in a urine sample.

Tables 3. The recovery of the spiked uric concentrations in the urine sample

Sample	Added Uric acid (mg/ml)	Found (mg/ml	% Recovery
Urine	0.00	ND	ND
	0.05	0.054	108.0
	0.07	0.069	98.60

Note: ND – not detected

Conclusion

This study has successfully synthesized fluorescent SiQDs using a one-pot hydrothermal method with APTES as a silicon source, trisodium citrate as a reducing agent, and ethylene diamine as a capping agent, respectively. Under optimized conditions, the fluorescence sensor response towards uric acid in the concentration range of 0.004 to 0.100 mg/ml gave good linearity ($y = 233467x + 3599.2$, $R^2 = 0.980$) and the LOD of 0.003 mg/ml. Notably stable and water-soluble, the resulting SiQDs hold promise for applications in biological contexts and healthcare sensing. The SiQDs provide valuable insights into their advantageous properties and potential applications in the field of nanomaterials and nanotechnology.

Acknowledgment

The authors would like to express gratitude to Universiti Putra Malaysia for providing sponsorship under the Putra Grant (GP-IPS/2023/9746800).

Author Contributions

Hassan Grema: Conceptualization, Methodology, Investigation, Writing – Original Draft. Jaafar Abdullah: Supervision, Conceptualization, Funding Acquisition, Writing – Review & Editing. Nor Azah Yusof: Supervision, Validation, Writing – Review & Editing.

Conflict of Interest

The authors declare that they have no known competing financial interests or personal relationships that could have appeared to influence the work reported in this paper.

Declaration of the Use of Generative AI

During the preparation of this work, the authors used AI-assisted tools (ChatGPT) for language polishing and grammatical refinement. After using this tool, the authors reviewed and edited the content as needed and take full responsibility for the content of the publication.

References

Agarwal, K., Rai, H., & Mondal, S. (2023). Quantum dots: An overview of synthesis, properties, and applications. *Materials Research Express, 10*. https://doi.org/10.1088/2053-1591/acda17

Azmi, N. E., Rashid, A. H. A., Abdullah, J., Yusof, N. A., & Sidek, H. (2018). Fluorescence biosensor based on encapsulated quantum dots/enzymes/sol-gel for non-invasive detection of uric acid. *Journal of Luminescence*, *202*, 309–315. https://doi.org/10.1016/j.jlumin.2018.05.075

Azizi, N., Hallaj, T., & Samadi, N. (2024). A dual-mode fluorometric and smartphone-based colorimetric sensor for cyanide detection using tungsten disulfide quantum dots and silver nanoparticles. *Journal of Food Composition and Analysis*, *129*, 106081. https://doi.org/10.1016/j.jfca.2024.106081

Baig, N., Kawde, A. N., & Elgamouz, A. (2022). A cost-effective disposable graphene-based sensor for sensitive and selective detection of uric acid in human urine. *Biosensors and Bioelectronics: X*, *11*, 100205. https://doi.org/10.1016/j.biosx.2022.100205

Eda, H., Kara, Ş., DemİrhanB., & DemİrhanB. E. R. (2020). Highly luminescent water-dispersed silicon quantum dots for fluorometric determination of oxytetracycline in milk samples. *Turkish Journal of Chemistry*, *44*, 1713–1722. https://doi.org/10.3906/kim-2007-4

Erden, P. E., & Kiliç, E. (2013). A review of enzymatic uric acid biosensors based on amperometric detection. *Talanta*, *107*, 312–323. https://doi.org/10.1016/j.talanta.2013.01.043

Kim, J., Imani, S., Araujo, W. R. De, Warchall, J., Valdés-ramírez, G., Paixão, T. R. L. C., Mercier, P. P., & Wang, J. (2015). Wearable salivary uric acid mouthguard biosensor with integrated wireless electronics. *Biosensors and Bioelectronic*, *74*, 1061–1068. https://doi.org/10.1016/j.bios.2015.07.039

Li, W., Liu, D., Dong, D., & You, T. (2021). Microwave-assisted synthesis of fluorescent silicon quantum dots for ratiometric sensing of Hg (II) based on the regulation of energy transfer. *Talanta*, *226*, 122093. https://doi.org/10.1016/j.talanta.2021.122093

Li, Y., Li, W., Zhang, H., Liu, Y., & Lei, B. (2020). Amplified light harvesting for enhancing Italian lettuce photosynthesis using water soluble silicon quantum dots as artificial antennas. *Nanoscale*, *12*, 155–166. https://doi.org/10.1039/c9nr08187a

Liu, Y., Cao, L., Zan, M., Peng, J., Wang, P., & Pang, X. (2021). Cyan-emitting silicon quantum dots as a fluorescent probe directly used for highly sensitive and selective detection of chlorogenic acid. *Talanta*, *233*, https://doi.org/10.1016/j.talanta.2021.122465

Liu, Y., Luo, S., Wu, P., Ma, C., Wu, X., Xu, M., & Li, W. (2019). Hydrothermal synthesis of green fl uorescent nitrogen doped carbon dots for the detection of nitrite and multicolor cellular imaging. *Analytica Chimica Acta*, *1090*, 133–142. https://doi.org/10.1016/j.aca.2019.09.015

Liu, Y., Zan, M., Cao, L., Peng, J., Wang, P., & Pang, X. (2022). F-doped silicon quantum dots as a novel fluorescence nanosensor for quantitative detection of new coccine and application in food samples. *Microchemical Journal*, *179*, https://doi.org/10.1016/j.microc.2022.107453

Miao, X., Yan, X., Qu, D., Li, D., Tao, F. F., & Sun, Z. (2017). Red emissive sulfur, nitrogen codoped carbon dots and their application in ion detection and theraonostics. *ACS Applied Materials and Interfaces*, *9*(22), 18549–18556. https://doi.org/10.1021/acsami.7b04514

Morozova, S., Alikina, M., Vinogradov, A., & Pagliaro, M. (2020). Silicon quantum dots: Synthesis, Encapsulation, and application in light-emitting diodes. *Frontiers in Chemistry*, *8*, 1–8. https://doi.org/10.3389/fchem.2020.00191

Pan, C., Qin, X., Lu, M., & Ma, Q. (2022). Water soluble silicon nanoparticles as a fluorescent probe for highly sensitive detection of rutin. *ACS Omega*, *7*, 28588–28596. https://doi.org/10.1021/acsomega.2c03463

Peng, Y., Shao, F., Guo, K., Zhuo, H., Wang, Y., Xie, X., & Tao, Y. (2022). SiQDs/Cu_2-β-CD nanoclusters: A fluorescence probe for the mutual non-interference detection of uric acid and L -cysteine under alkaline conditions. *Inorganic Chemistry Communications*, *143*, 109765. https://doi.org/10.1016/j.inoche.2022.109765

Pleskacova, A., Brejcha, S., Pacal, L., Kankova, K., & Tomandl, J. (2016). Simultaneous determination of uric acid, xanthine and hypoxanthine in human plasma and serum by HPLC–UV: Uric acid metabolism tracking. *Chromatographia*, *80*(4), 529–536. https://doi.org/10.1007/s10337-016-3208-8

Schrenkhammer, P. (2008). New optical biosensors for uric acid and glucose new optical biosensors for uric acid and glucose, Doctoral Thesis, University of Regensburg

Stephan, T., & Trappitsch, R. (2023). Reliable uncertainties: Error correlation, rotated error bars, and linear regressions in three-isotope plots and beyond. *International Journal of Mass Spectrometry*, *491*, 117053. https://doi.org/10.1016/j.ijms.2023.117053

Tatli, F., Calam, T. T., Uzun, D., & Hasdemir, E. (2020). The determination of uric acid in the presence of ascorbic acid and dopamine using [(1H-1,2,4-triazole-3-ylimino)methyl]naphthalene-2-ol modified platinum electrode. *Journal of the Faculty of Engineering and Architecture of Gazi University*, *35*(4), 2013–2022. https://doi.org/10.17341/gazimmfd.525552

Tukimin, N., Abdullah, J., & Sulaiman, Y. (2017). Development of a PrGo-modified electrode for uric acid determination in the presence of ascorbic acid by an electrochemical technique. *Sensors*, *17*(7). https://doi.org/10.3390/s17071539

Wang, Y., Yang, Y., Liu, W., Ding, F., Zhao, Q., Zou, P., Wang, X., & Rao, H. (2018). Colorimetric and fluorometric determination of uric acid based on the use of nitrogen-doped carbon quantum dots and silver triangular nanoprisms. *Microchimica Acta*, *185*(6). https://doi.org/10.1007/s00604-018-2814-6

Westley, C., Xu, Y., Thilaganathan, B., Carnell, A. J., Turner, N. J., & Goodacre, R. (2017). Absolute quantification of uric acid in human urine using surface enhanced Raman scattering with the standard addition method. *Analytical Chemistry*, *89*, 2472–2477. https://doi.org/10.1021/acs.analchem.6b04588

Wu, J., Dai, J., Shao, Y., & Sun, Y. (2015). One-step synthesis of fluorescent silicon quantum dots (Si-QDs) and their application for cell imaging. *RSC Advances*, *5*(102), 83581–83587. https://doi.org/10.1039/c5ra13119g

Xu, D., Lei, F., Chen, H., Yin, L., Shi, Y., & Xie, J. (2019). One-step hydrothermal synthesis and optical properties of self-quenching-resistant carbon dots towards fluorescent ink and as nanosensors for Fe^{3+} detection. *RSC Advances*, *9*, 8290–8299. https://doi.org/10.1039/C8RA10570G

Xuan, T., Yang, X., Lou, S., Huang, J., Liu, Y., Yu, J., Li, H., Wong, K., Wang, C., & Wang, J. (2017). Highly stable $CsPbBr_3$ quantum dots coated with alkyl phosphate for white light-emitting diodes. *Nanoscale*, *9*, 15286–15290. https://doi.org/10.1039/c7nr04179a

Yaacob, A., Ngajikin, N. H., Rashid, N. C. A., Ali, S. H. A., Yaacob, M., Isaak, S., & Cholan, N. A. (2020). Uric acid detection in visible spectrum. *TELKOMNIKA Telecommunication, Computing, Electronics and Control*, *18*(4), 2035–2041. https://doi.org/10.12928/TELKOMNIKA.V18I4.14993

Zhang, Z., Wang, L., Wang, J., Jiang, X., Li, X., Hu, Z., Ji, Y., Wu, X., & Chen, C. (2012). Mesoporous silica-coated gold nanorods as a light-mediated multifunctional theranostic platform for cancer treatment. *Advanced Materials*, *24*, 1418–1423. https://doi.org/10.1002/adma.201104714

Zheng, Q., Xiong, L., Yu, L., Wu, D., Yang, C., & Xiao, Y. (2021). An enzyme-free fluorescent sensing platform for the detection of uric acid in human urine. *Journal of Luminescence*, *236*, 1–8. https://doi.org/10.1016/j.jlumin.2021.118076

Zhou, Y., Qi, M., & Yang, M. (2022). Fluorescence determination of lactate dehydrogenase activity based on silicon quantum dots. *Spectrochimica Acta Part A: Molecular and Biomolecular Spectroscopy*, *268*, 120697. https://doi.org/10.1016/j.saa.2021.120697